Available online at www.sciencedirect.com
SCIENCE DIRECT®
Optics Communications 260 (2006) 528–534
OPTICS COMMUNICATIONS
www.elsevier.com/locate/optcom

Temporal Talbot effect applied to determine dispersion parameters

Christian Cuadrado-Laborde [a,*], Pablo A. Costanzo-Caso [a], Ricardo Duchowicz [a], Enrique E. Sicre [b]

[a] Centro de Investigaciones Ópticas (CIOp) and Facultad de Ciencias Exactas (UNLP), Camino Centenario entre 505 y 508, Casilla de Correo 124, (1900) La Plata, Argentina
[b] Centro de Estudios Avanzados (CEAV), Universidad Argentina de la Empresa (UADE), Chile 1192, (1073) Buenos Aires, Argentina

Received 30 June 2005; received in revised form 27 October 2005; accepted 29 October 2005

Abstract

The space–time duality theory and the temporal selfimaging phenomenon (or Talbot effect) are used to propose a method for determining dispersion parameters associated with an optic fiber link. From the space–time analogy, the actions of free-space propagation and phase curvatures taking place in the general spatial Talbot effect are implemented for time-varying wavefields. Using the temporal selfimaging conditions, a relationship is derived for determining the second-order dispersion coefficient of a given dispersive medium under test. As a particular application, we analyze the feasibility of the measuring approach using a linearly chirped fiber grating as the dispersive component under test. Some simulations are carried out in order to study the sensitivity and accuracy of the developed method.

Keywords: Temporal Talbot effect; Pulse transmission; Dispersion

1. Introduction

The space–time duality is based on the close mathematical analogy between the impulse response equations describing paraxial diffraction of optical beams in free-space propagation and temporal distortion of light pulses traveling in dispersive media, i.e., linearly chirped fiber gratings (LCFGs) or optical fibers [1–11]. In the space domain, the Talbot effect, or selfimaging phenomenon, is a well-known optical experiment, which has been widely studied [12,13]. Several applications have been developed in different fields such as interferometry, metrology and image processing [14]. Using the space–time duality relationships, it was proposed the temporal analogue of the Talbot effect for light transmission in single mode optical fibers [15–19]. As a direct application of this phenomenon, periodic pulse trains with minimum distortion and different repetition periods can be obtained.

In this paper, we propose an application of the temporal Talbot effect to implement a method for determining the second-order dispersion coefficient of a certain dispersive device under test. Although the basic relationships of the method are derived for a quite general case, we focus our attention to consider the particular case of the LCFGs. Since these components become quite useful in the development of dispersion compensation techniques, an accurate measurement approach of the LCFG dispersion parameters is an application of great concern in the field of long-haul, optical communication systems [20]. Most of the well-known techniques for measuring chromatic dispersion, such as the modulation phase-shift and the pulse delay methods [21], determine the group delay changes corresponding to different wavelength intervals. In this way, they suit properly for characterizing fiber optic dispersion but are not so adequate for the dispersion measurement of the LCFG since the wavelength range (in reflection) is very narrow in this case.

* Corresponding author. Tel.: +54 0221 4840280; fax: +54 0221 4712771.
E-mail addresses: claborde@ciop.unlp.edu.ar (C. Cuadrado-Laborde), ricardod@ciop.unlp.edu.ar (R. Duchowicz), esicre@uade.edu.ar (E.E. Sicre).

0030-4018/$ - see front matter © 2005 Elsevier B.V. All rights reserved.
doi:10.1016/j.optcom.2005.10.073

In the general spatial Talbot effect, a periodic grating is illuminated with a spherical wavefront. The diffracted field becomes scaled replica of the input periodic structure at certain fixed locations. In the temporal analogue experiment, a periodic pulse train replaces the grating structure, a time lens does the spherical wave illumination action and the free-space propagation is realized by pulse transmission in a certain dispersive medium. In the proposed optical device, the output signal becomes a replica of the input pulse train but with a different repetition rate, which depends on both the phase modulation factor and the dispersion parameter of the LCFG [18]. Using the temporal Talbot conditions, we derive a relationship for obtaining the second-order dispersion coefficient of the LCFG under study. Some simulations are done for illustrating the presented approach. The measuring sensitivity and the involved errors of the method are analyzed, followed by a discussion concerning with the required (realizable) time lenses that are needed for a practical implementation of the method.

2. Space–time analogy applied to temporal selfimaging

The general problem of selfimaging in the temporal domain was extensively treated by Azaña and Chen [18]. Based on this analysis, let us consider the basic relationships involved in the selfimage formation in order to be further employed for implementing the dispersion measuring method. In the spatial Talbot effect, a periodic object G is illuminated with a spherical wavefront of wavelength λ. This situation becomes equivalent to employ planewave illumination and to insert a lens L (just behind G) of focal length f. Depending on the lens (if positive or negative), G is illuminated with a convergent or a divergent spherical wave, respectively. Thus, the selfimaging formation can be considered as a tandem operation on the periodic input amplitude of lens action plus free-space propagation. For certain distances $z = z_T$, the diffracted field amplitude $u(x;z)$ becomes scaled replicas of G; i.e.,

$$u(x; z_T) = u_{in}(x/M; 0), \tag{1a}$$

$$z_T = n\frac{Md^2}{\lambda}, \tag{1b}$$

where the scaling factor M of the selfimage located at z_T is given by

$$M = \frac{f + z_T}{f}, \tag{2}$$

being d the spatial period of G and n an arbitrary integer. It should be noted that: (i) for $z > 0$, the scale factor is $M > 1$ for $f > 0$, and $M < 1$ for $f < 0$; (ii) the Talbot distances z_T are not equidistant since the magnification factor M depends on z_T itself. At other specific distances from G given as

$$z_{T,m} = \frac{n}{m}\frac{Md^2}{\lambda}, \tag{3}$$

where n, m are coprime integers (and $m \geqslant 2$), a periodic pattern is reobtained but now the period d_m of these so-called fractional Talbot selfimages is also modified by the integer m as

$$d_m = \frac{Md}{m}. \tag{4}$$

The duty-cycle a/d associated with the input periodic pattern G (being a the slit width) remains unchanged for the integer Talbot selfimages, but it is modified as $m \times (a/d)$ for the fractional selfimages. This effect becomes the main difference between integer and fractional Talbot effects, and it imposes a restriction to the allowed values of m for which the fractional selfimages can be actually visualized.

In the temporal domain, a time lens introduces a quadratic phase modulation into the time-varying signal. Besides, a dispersive medium (up to the first-order) has associated a quadratic-phase spectral response with a mathematical expression similar to that found in spatial Fresnel diffraction. Therefore, space–time equivalencies can be established as [6,7]

$$\lambda z \Longleftrightarrow 2\pi\Phi_{20}, \tag{5a}$$

$$\frac{2\pi}{\lambda f} \Longleftrightarrow \phi_{20}, \tag{5b}$$

where Φ_{20} is the second-order dispersion coefficient of the medium (specified at the working central frequency $\omega = \omega_0$) and ϕ_{20} is the quadratic modulation factor of the time lens. By applying this space–time analogy, and taking into account the spatial Talbot effect (Eqs. (1)–(4)), the equivalent temporal selfimaging conditions can be derived. Thus, if a periodic input pulse train with repetition period T_0 is initially phase-modulated, as given by Eq. (5b), and then it is transmitted through a first-order dispersive medium (Eq. (5a)), the output signal becomes a scaled replica of the input pulse train irradiance whenever the involved parameters are related as [18]

$$|\Phi_{20}| = \frac{n}{m}\frac{T_0^2}{2\pi}|1 - \Phi_{20}\phi_{20}|, \tag{6}$$

being the repetition period T of the output selfimage

$$T = |1 - \Phi_{20}\phi_{20}|\frac{T_0}{m}. \tag{7}$$

where n, m are coprime integers. For $m = 1$ the integer Talbot effect is observed, and for $m \geqslant 2$ the fractional. However, this fractional Talbot effect is only observed if the output pulses do not temporally overlap.

3. Dispersion determination based on the temporal Talbot effect

The optical arrangement proposed to implement the dispersion measuring technique is shown in Fig. 1. A periodic sequence of light pulses, with arbitrary shape and repetition period T_0, propagates in a single mode optical fiber. This input signal successively interacts with a phase modulator (time lens) and with the dispersive medium under test,

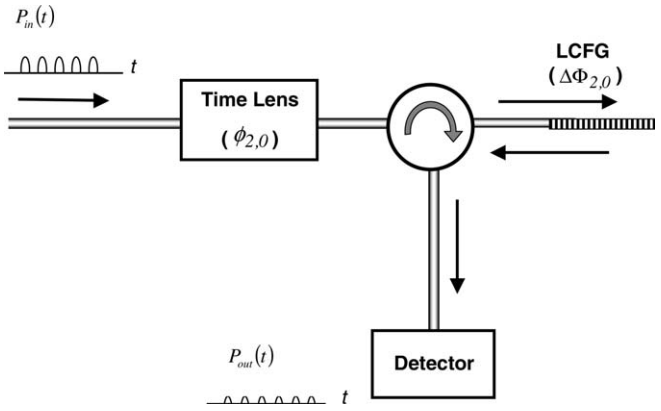

Fig. 1. Scheme of the proposed optical device. LCFG is the linearly chirped fiber grating under test. OC is an optical circulator.

which can be either an optical fiber or a LCFG. In this last case, the properties of the reflected signal amplitude are determined by the reflection coefficient $r(\Delta\omega)$ associated with the LCFG, which, in the proximity of the central Bragg frequency ω_0, can be written as

$$r(\Delta\omega) = r_0 \exp(-i\Delta\Phi_{10}\Delta\omega) \times \exp\left[-i\frac{\Delta\Phi_{20}}{2}(\Delta\omega)^2\right] \exp\left[-i\Phi_r(\Delta\omega)\right], \quad (8)$$

being $\Delta\omega = \omega - \omega_0$ the frequency difference variable and $\Delta\Phi_{k0} = (\partial^k\Phi/\partial\omega^k)\omega_0$, with $k = 1,2$, the k-order derivatives of the phase function $\Phi(\omega)$ associated with the LCFG, both calculated at $\omega = \omega_0$. An additional phase term $\Phi_r(\Delta\omega)$ was included in Eq. (8) to take into account the ripple in the group delay, which is normally present in a LCFG unless an apodization procedure is to be implemented. It should be noted that Eq. (8) could also describe the pulse train propagation through an optical fiber (now as a transmission transfer function), where $\Phi_r(\Delta\omega)$ takes into account the effect of the third-order fiber dispersion. From now on, we restrict the analysis to the LCFGs being the method also applicable to optical fibers in a similar way. Inside a certain limited spectral bandwidth $\delta\omega$, centered at $\omega = \omega_0$, the coefficients $\Delta\Phi_{k0}$ can be considered as nearly constant and $|r(\Delta\omega)| = r_0$ is the reflectivity for $\omega = \omega_0$. The spectral behavior of the reflected light pulse is determined by $r(\Delta\omega)$ so it can be considered as the transfer function of the pulse train reflected by the LCFG. If we neglect the effect of $\Phi_r(\Delta\omega)$, the transfer function of the LCFG becomes similar to the dispersion line used to establish the space–time equivalency (as given by Eq. (5a)) replacing the coefficient $\Delta\Phi_{20}$ by Φ_{20}. The effects due to the ripple in the group delay of the LCFG, or to the third-order dispersion in the case of a fiber, will be later studied in this section. Since $\Delta\Phi_{20} > 0$ for the case of a LCFG, depending on ϕ_{20} (if positive or negative), the output signal can be a magnified temporal selfimage (by selecting $|1-\Delta\Phi_{20}\phi_{20}| > 1$) or a compressed temporal selfimage (by selecting $|1-\Delta\Phi_{20}\phi_{20}| < 1$), whenever the integer Talbot condition is satisfied. In this instance, from Eq. (7) the repetition period T of the output pulse train becomes

$$T = |1 - \Delta\Phi_{20}\phi_{20}|T_0 = MT_0, \quad (9)$$

being $M = |1-\Delta\Phi_{20}\phi_{20}|$ the selfimage magnification.

We propose the following measurement procedure. First, for a given fixed quadratic phase modulation factor ϕ_{20}, the repetition period T_0 of the input pulse train is varied in such a way that the output signal becomes a temporal integer selfimage, which means that the Talbot condition, as established by Eq. (6) for $m = 1$, is satisfied. The repetition period T of the output irradiance is measured, and the selfimage magnification is obtained as $M = T/T_0$. From Eq. (9), the unknown dispersion coefficient $\Delta\Phi_{20}$ associated with the LCFG results as

$$\Delta\Phi_{20} = \left|\frac{1-M}{\phi_{20}}\right|. \quad (10)$$

Since the dispersion coefficient is obtained from an integer Talbot condition, it becomes important to distinguish between integer and fractional selfimaging. If the output signal is detected for a certain fractional selfimaging condition and the period T is measured, then an uncertainly originated by the unknown integer m results, because $M = m \cdot T/T_0$ (from Eq. (7)). This uncertainly is translated to the determination of dispersion coefficient $\Delta\Phi_{20}$ from Eq. (10). Thus the sub-Talbot effect is not a convenient measurement condition. However, these fractional selfimages can be discarded by determining from the output irradiance both the repetition period T and its duty-cycle. As it was discussed in Section 2, the duty-cycle of the different magnified selfimages remains constant and equal to the duty-cycle associated with the input periodic pattern. On the contrary, the duty-cycle varies for the fractional selfimages proportional to the value of the integer m.

Next, for studying the accuracy of the method we analyze the involved errors measurement. Basically, we consider two components: (i) the error propagation in Eq. (10), from which the unknown dispersion coefficient $\Delta\Phi_{20}$ is derived, and (ii) the adjust error, or insensibility, due to the adjustment of an integer Talbot condition. Therefore small variations of T_0 will produce an output signal change that cannot be detected by the employed measuring instrument. From Eq. (10), the propagation error e_p results as

$$e_p = \frac{2M}{1-M}e_T, \quad (11)$$

being e_T the relative error involved in the time measurement.

For determining the second component (the adjust error), we assume a measurement situation near to an integer Talbot condition and we determine the minimum change in the input period, producing a detectable change in the output signal (which depends on the measurement capability of the instrument). Thus, by performing a combined error analysis involving Eq. (10) and the required duty-cycle conservation condition, the adjust error e_{ad} can be found as

$$e_{ad} = \frac{M}{1-M}\delta t, \quad (12)$$

where δt is the relative resolution of the instrument being used for time measurement. If the measurement condition is favorable, then satisfy $\delta t \ll e_T$, from Eqs. (11) and (12) it can be seen that $e_{ad} \ll e_p$, and so it can be neglected as compared with e_p.

As it was mentioned in the errors discussion above, it is important to accurately "recognize" a selfimaging condition, namely, by varying the input period T_0 we must decide when an output selfimage is met. We analyze this effect by determining the similarity degree existing between the input and output signals in the vicinity of a Talbot condition. To this end, we introduce a convolution parameter C defined as

$$C = \frac{\max\{I_{out} * I_{in}\}}{\max\{I_{out}\} \times \max\{I_{in}\}}, \tag{13}$$

where $\max\{\ldots\}$ denotes the maximum value of the function between each curly brackets and $I_{out} * I_{in}$ means convolution operation in the time domain between the irradiances of the output and input pulse trains. Thus, by detecting the output irradiance $I_{out}(t)$, the parameter C can be obtained by using Eq. (13). In Fig. 2, it is shown the variation of C for different repetition periods T_0 of the input pulse train, in a range between 40 and 150 ps. As it is expected, there exist several peaks associated with integer and fractional selfimages (the variation of the peaks height is due to the normalization procedure chosen in Eq. (13)). Since these peaks are very sharp, the selection of T_0 for obtaining a selfimaging condition can be accurately performed. This feature will be better illustrated in the following section with an application. On the other hand, if we compare the curve of Fig. 2 with the correlation curve that is shown in [16], which was obtained for the temporal Talbot effect without phase modulation, it can be observed broader correlation peaks. In our case the time lens effect makes easy the determination of T_0 that satisfy de integer Talbot condition.

To obtain the Talbot condition in order to determine the dispersion parameter, we have considered the LCFG characterized by a quadratic phase transfer function. The group delay ripple in the LCFG (or the third-order dispersion coefficient if an optical fiber were considered) produces an additional phase term $\Phi_r(\Delta\omega)$, which was neglected in the analysis following Eq. (8). Let us now to discuss the validity of this approximation evaluating the effect of the group delay ripple on the periodic pulse train when the integer Talbot condition is achieved. The practical LCFGs, which are commonly used for single channel dispersion compensation, have associated a chirp parameter in the range 0.03–0.1 nm/cm and a fiber distance between 1 and 40 cm [22]. In these gratings, the amplitude of the group delay ripple never reaches the 200 ps, and the maximum oscillation periodicity is around 5 GHz (these represents the worst conditions). Fig. 3 shows the output signal (at a Talbot condition) when the group delay ripple is considered (dotted line), and without including $\Phi_r(\Delta\omega)$ (solid line). The ripple was considered with amplitude of 200 ps and 5–1 GHz linearly variable interval of oscillation, inside a bandwidth of 100 GHz centered at the Bragg central frequency. In Fig. 3(a), the ripple effect is practically not observed. In Fig. 3(b), a small time interval of the output signal was amplified so it can be observed low distortion amplitude, which is around two-order of magnitude lower than the original pulse amplitude. Thus, we conclude that the Talbot selfimage remains almost unchanged, so justifying the selection of a quadratic phase transfer function for the pulse reflection analysis in the LCFG. Indeed, it was experimentally demonstrated the excellent performance of a LCFG as a real time Fourier transformer [9].

Finally, for the case of pulse transmission in standard optical fibers, Fatome et al. [23] studied, from a theoretical and experimental point of view, the behavior of a periodic pulse train, satisfying the Talbot conditions, under the influence of the third order dispersion. They showed that

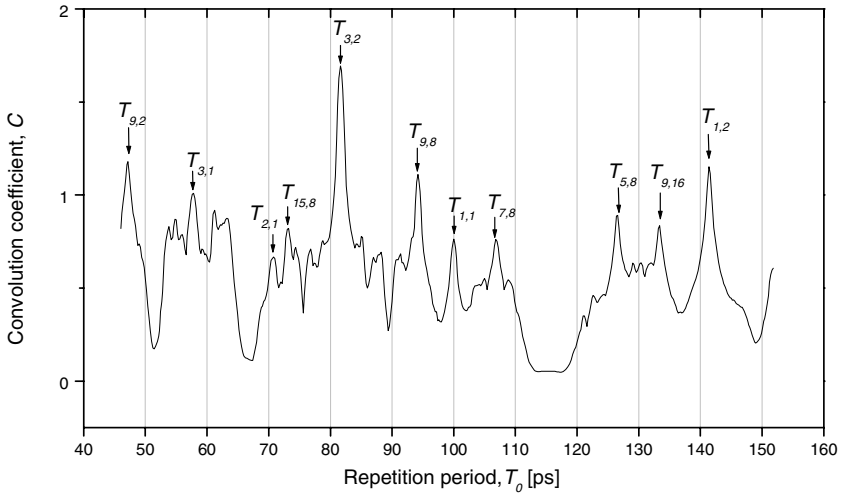

Fig. 2. Convolution parameter C vs. period T_0 of the input pulse train. $T_{n,m}$ denotes each convolution peak whenever T_0 satisfy a Talbot condition. The integer selfimaging corresponds to $n = m$, whereas the functional selfimaging appears for $n \neq m$. The height variation of the several peaks is due to the normalization procedure chosen for C.

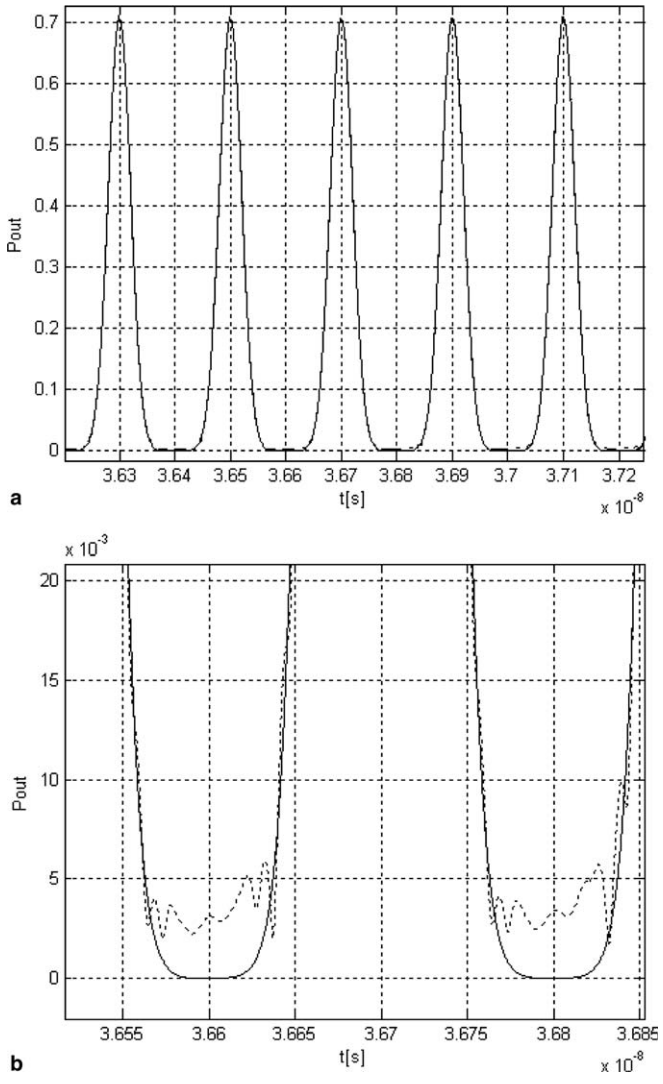

Fig. 3. Ripple effect of a LCFG on the output optical irradiance using the setup of Fig. 1: (a) output signal (at a Talbot condition) when the group delay ripple is considered (dotted line) and without considering this effect (solid line); (b) a small time interval of the output signal was amplified so it can be observed the low distortion amplitude introduced by this effect.

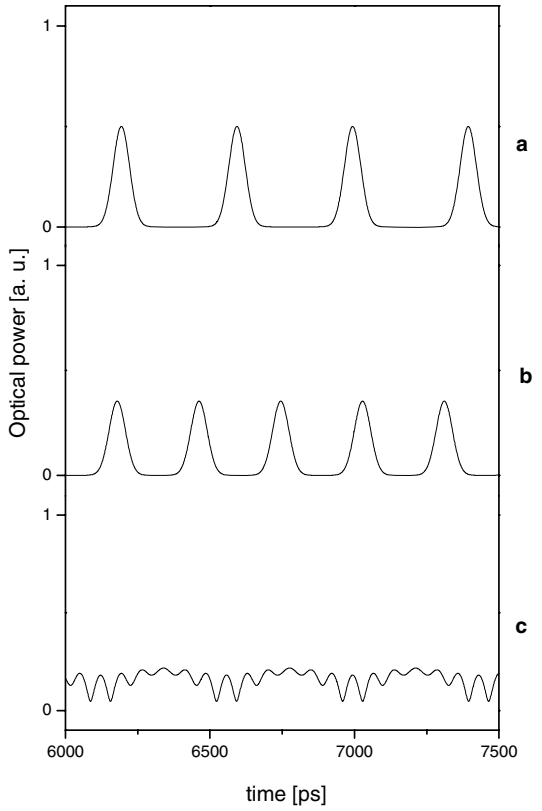

Fig. 4. Output optical irradiance using the setup of Fig. 1: (a) the selfimaging condition is satisfied with: $T_0 = 100$ ps ($T_{n=1,m=1}$, in the convolution curve); (b) a fractional selfimaging condition is found with: $T_0 = 141.4$ ps ($T_{n=1,m=2}$, in the convolution curve). A change in the duty-cycle can be clearly observed; (c) the selfimaging condition is not satisfied with: $T_0 = 109$ ps. A large distortion of the pulse train can be observed.

third order dispersion effects are noticeable whenever the repetition rate is high enough ($T_0 < 6$ ps), a situation which is not to be selected in our method (where $T_0 \cong 100$ ps), as we illustrate in the following section with some examples.

4. Applications and results

In order to illustrate the proposed approach, we numerically calculate the light propagation through the optical device schematized in Fig. 1. The input pulse train was initially built as $N = 41$ consecutive light pulses each one separated by a time interval T_0. The later was varied maintaining the pulse width constant to a value FWHM = 16.7 ps. This input signal successively interacts with a phase modulator initially characterized with a $\phi_{20}^{(1)} = -4.7124 \times 10^{20}$ Hz^2 rad and finally with a LCFG having dispersion coefficients: $\Delta\Phi_{10} = 1$ ns, $\Delta\Phi_{20} = 6.36 \times 10^3$ ps^2/rad, being the Bragg central frequency $v_0 =$ 193.165 THz. In Fig. 4, the output irradiances are shown for three different situations: (a) the output signal becomes a Talbot selfimage, with $n = 1$, being the repetition period $T_0 = 100$ ps; (b) the output signal becomes a fractional selfimage, with $n = 1$ and $m = 2$, being the repetition period $T_0 = 141{,}4$ ps (in this case the output pulse width is the same as in case (a) but not the period T so originating a change of the duty-cycle); (c) the input period was selected as $T_0 = 109$ ps (which does not satisfy the Talbot condition, integer or fractional), so it can be observed a strong distortion of the pulse train.

Now, the measuring capability of the method will be tested using the quadratic phase modulation factor mentioned above ($\phi_{20}^{(1)} = -4.7124 \times 10^{20}$ Hz^2 rad), and a new one ($\phi_{20}^{(2)} = -(1/4)\phi_{20}^{(1)} = 1.1781 \times 10^{20}$ Hz^2 rad). These values were selected in order to get two well distinct cases: $M > 1$ (for $\phi_{20}^{(1)}$) and $0 < M < 1$ (for $\phi_{20}^{(2)}$). Fig. 5(a) (for $\phi_{20}^{(1)}$) and Fig. 5(b) (for $\phi_{20}^{(2)}$) show the several calculation points (and the interpolating curves) that are obtained by varying the repetition period T_0, and for a wide range of values of the dispersion coefficient $\Delta\Phi_{20}$ (which is the parameter to be derived). As $\Delta\Phi_{20}$ is obtained (see Eq. (10)) by determin-

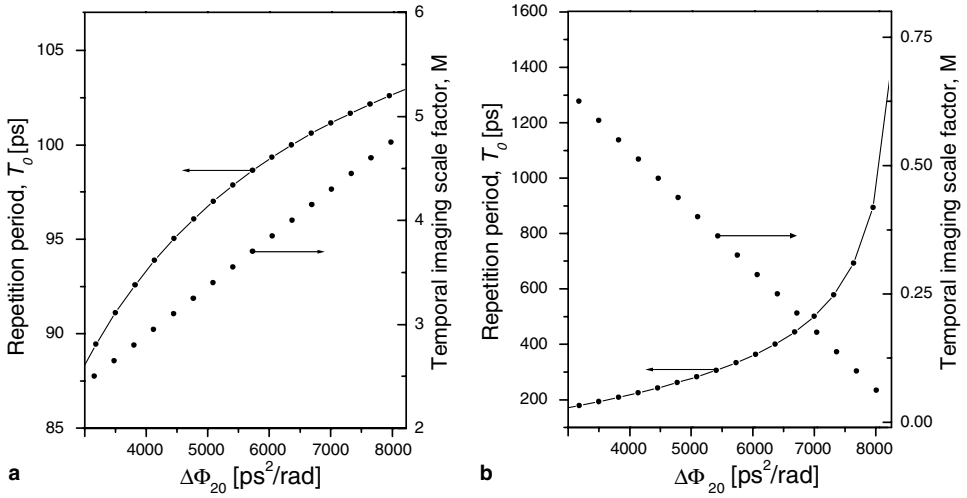

Fig. 5. Results obtained from the numerical calculations. The solid curves passing through the calculated values give the variation of the input period T_0 with the dispersion coefficient $\Delta\Phi_{20}$ to be determined. The calculated values (the symbols alone) give the linear relationship between the selfimage period magnification M and $\Delta\Phi_{20}$. In all cases, the integer selfimage condition with $n = 1$ is satisfied. The calculations were repeated for two phase modulation factors: (a) $\phi_{20}^{(1)} = -4.7124 \times 10^{20}$ Hz^2 rad, and (b) $\phi_{20}^{(2)} = -(1/4)\phi_{20}^{(1)} = 1.1781 \times 10^{20}$ Hz^2 rad.

ing the selfimage magnification M, these values are also included in the right side, vertical axis (points without an interpolation line). The solid line curves passing through the several calculation points illustrate the variation of T_0 for the different dispersion parameters $\Delta\Phi_{20}$, while the points alone (depicting a linear variation, in accordance with Eq. (9)) illustrate the change of the selfimage magnification M for varying $\Delta\Phi_{20}$.

We now analyze the uncertainty involved in the determination of the dispersion coefficient $\Delta\Phi_{20}$. By considering $\phi_{20}^{(1)}$, the Talbot selfimage (for $n = 1$) is obtained for a repetition period $T_0 = 100$ ps. As it was previously discussed, the main error measurement is given by Eq. (11), with e_T as the relative error of the time measurement. Therefore, the whole measuring uncertainty can be described by Eq. (11). By considering $e_T \cong 1\%$, and taking into account that $M = 4$, it results a relative error in the $\Delta\Phi_{20}$ determination of $e_p \cong 2.7\%$. An identical consideration in the case of $\phi_{20}^{(2)}$ results in a relative error in the $\Delta\Phi_{20}$ determination of $e_p \cong 0.7\%$. These values may be compared with that obtained by the method proposed by Azaña and Muriel employing selfimaging in a two steps measuring procedure [16]. In this case, for the same value of the dispersion coefficient, the relative error can be estimated as $e_p \sim 10\%$. Thus, the time lens effect (changing the selfimage magnification) allows achieving high sensitivity and a low relative error measurement.

The optical implementation feasibility of the method will be now discussed. The effects of chirped laser pulse sequences on temporal selfimaging phenomena have been recently discussed [24]. Besides this, the effect of the time lens is critical, and here we discuss some of its properties. If we assume that the time lens is realized by an electro-optic phase modulator driven with a sinusoidal voltage of angular frequency ω_m, then the optical wave form must be shorter than a time aperture: $TA \sim 1/\omega_m$, with $\omega_m \sim (\phi_{20})^{1/2}$ [4]. Thus, by employing this technology, phase factors and time apertures are related by: $TA \sim (|\phi_{20}|)^{-1/2}$. For $\phi_{20}^{(1)} = -4.7124 \times 10^{20}$ Hz^2 rad, it is obtained: $TA_1 \cong 50$ ps and so it is not possible to select $N = 41$ pulses with $T_0 = 100$ ps, because this input train exceeds the obtained time aperture. Similar considerations with $\phi_{20}^{(2)} = 1.1781 \times 10^{20}$ Hz^2 rad results in a time aperture: $TA_2 \cong 90$ ps. Although $TA_2 > TA_1$, the second input train (for the $\phi_{20}^{(2)}$ case) is four times longer, for identical N (Fig. 5), this clearly represents a worst situation. Therefore, it is important to know how the selfimage formation is affected by reducing the time duration of the input train, namely N. To this end we recalculate the convolution parameter C, as given by Eq. (13), by diminishing N. From Fig. 6, it can be observed that $N = 15$ pulses would be an

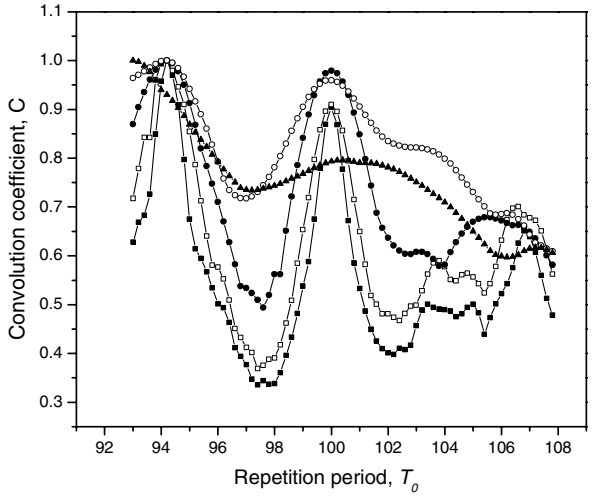

Fig. 6. Convolution parameter curves around an integer Talbot condition ($n = 1$, $T_0 = 100$ ps) for different input pulse number: $N = 41$ (solid square), $N = 31$ (open square), $N = 21$ (solid circle), $N = 15$ (open circle) and $N = 11$ (solid triangle).

acceptable minimum. Therefore, we need to modulate at least 15 consecutive light pulses each one separated by 100 ps (400 ps), for the $\phi_{20}^{(1)}(\phi_{20}^{(2)})$ numerical example. However, with time lens based on sum-frequency generation in a non-linear crystal, these limitations can be overcame, and the time lens can be selected to provide the selected phase factor and time aperture, essentially as independent parameters [25,26]. To conclude we believe that this time lens technology based on non-linear processes would be an optimal candidate to implement this measurement procedure.

5. Conclusions

In this paper, we presented a method based on the temporal Talbot effect for determining the dispersion parameter associated with a LCFG. By combining a quadratic phase modulation action on a periodic, input pulse train together with propagation/reflection in the dispersive component (LCFG), output periodic pulse trains having minimum distortion and different magnified repetition rates can be obtained. The unknown dispersion coefficient of the LCFG can be determined by obtaining the magnification factor of the period associated with the output temporal selfimage. In order to avoid fractional (or sub-Talbot) selfimaging, which would difficult the determination of the dispersion value, a criterion is given based on the detection of the selfimage duty-cycle. The uncertainty in the dispersion determination, inherent to the proposed method, was analyzed. From the numerical simulations performed, it can be attained a relative error below 3% (for $M = 4$) which is very adequate for most dispersion compensation techniques.

Acknowledgements

This research was financially supported by Universidad Argentina de la Empresa (UADE), Consejo Nacional de Investigaciones Científicas y Técnicas (CONICET-PIP2950/04) and Facultad de Ingeniería, Universidad Nacional de La Plata (UNLP-Project I106), Argentina. CCL is fellow of CONICET and PCC is fellow of Comisión de Investigaciones Científicas de la Pcia. de Buenos Aires (CIC). The authors thank the anonymous reviewers for their helpful comments.

References

[1] E.B. Treacy, IEEE J. Quantum Electron. QE-5 (1969) 454.
[2] T. Jannson, J. Jannson, J. Opt. Soc. Am. 71 (1981) 1373.
[3] T. Jannson, Opt. Lett. 8 (1983) 232.
[4] B.H. Kolner, M. Nazarathy, Opt. Lett. 14 (1989) 630.
[5] A.W. Lohmann, D. Mendlovic, Appl. Opt. 31 (1992) 6212.
[6] B.H. Kolner, IEEE J. Quantum. Electron. 30 (1994) 1951.
[7] A. Papoulis, J. Opt. Soc. Am. A 11 (1994) 3.
[8] P. Naulleau, E. Leith, Appl. Opt. 34 (1995) 4119.
[9] M.A. Muriel, J. Azaña, A. Carballar, Opt. Lett. 24 (1999) 1.
[10] J. Azaña, L.R. Chen, M.A. Muriel, P.W.E. Smith, Electron. Lett. 35 (1999) 2223.
[11] F. Ouellette, Opt. Lett. 12 (1987) 847.
[12] Lord Rayleigh, Philos. Mag. 11 (1881) 196.
[13] J.T. Winthrop, C.R. Worthington, J. Opt. Soc. Am. 55 (1965) 373.
[14] K. Patorski, in: E. Wolf (Ed.), Progress in Optics, XXVII, Elsevier, Amsterdam, 1989, p. 1.
[15] J. Azaña, M.A. Muriel, Opt. Lett. 24 (1999) 1672.
[16] J. Azaña, M.A. Muriel, Appl. Opt. 38 (1999) 6700.
[17] J. Azaña, J. Opt. Soc. Am. B 20 (2003) 83.
[18] J. Azaña, L.R. Chen, J. Opt. Soc. Am. B 20 (2003) 1447.
[19] E.E. Sicre, D. Zalvidea, R. Duchowicz, Appl. Opt. 43 (2004) 3005.
[20] G.P. Agrawal, Fiber-Optic Communication Systems, second ed., Wiley, New York, 1997.
[21] D. Derickson, Fiber Optic Test and Measurement, Prentice-Hall, New Jersey, 1998.
[22] R. Kashyap, Fiber Bragg Gratings, Academic Press, 1999 (Chapter 7).
[23] J. Fatome, S. Pitois, G. Millot, Opt. Commun. 234 (2004) 29.
[24] J. Lancis, J. Caraquitena, P. Andrés, M.A. Muriel, Opt. Commun. 253 (2005) 156.
[25] C.V. Bennett, B.H. Kolner, Opt. Lett. 24 (1999) 783.
[26] C.V. Bennett, B.H. Kolner, IEEE J. Quantum. Electron. 36 (2000) 649.